Ice nucleation and droplet formation by bare and coated soot particles

Beth Friedman,[1] Gourihar Kulkarni,[2] Josef Beránek,[2] Alla Zelenyuk,[2] Joel A. Thornton,[1] and Daniel J. Cziczo[2,3]

Received 25 March 2011; revised 16 June 2011; accepted 27 June 2011; published 13 September 2011.

[1] We have studied ice formation at temperatures relevant to homogeneous and heterogeneous ice nucleation, as well as droplet activation and hygroscopicity, of soot particles of variable size and composition. Coatings of adipic, malic, and oleic acid were applied in order to span an atmospherically relevant range of solubility, and both uncoated and oleic acid coated soot particles were exposed to ozone in order to simulate atmospheric oxidation. The results are interpreted in terms of onset ice nucleation, with a comparison to a mineral dust particle that acts as an efficient ice nucleus, and particle hygroscopicity. At 253 K and 243 K, we found no evidence of heterogeneous ice nucleation occurring above the level of detection for our experimental conditions. Above water saturation, only droplet formation was observed. At 233 K, we observe the occurrence of homogeneous ice nucleation for all particles studied. Coatings also did not significantly alter the ice nucleation behavior of soot particles but aided in the uptake of water. Hygroscopicity studies confirmed that pure soot particles were hydrophobic, and coated soot particles activated as droplets at high water supersaturations. A small amount of heterogeneous ice nucleation either below the detection limit of our instrument or concurrent with droplet formation and/or homogeneous freezing cannot be precluded, but we are able to set limits for its frequency. We conclude that both uncoated and coated soot particles comparable to those generated in our studies are unlikely to significantly contribute to the global budget of heterogeneous ice nuclei at temperatures between 233 K and 253 K.

Citation: Friedman, B., G. Kulkarni, J. Beránek, A. Zelenyuk, J. A. Thornton, and D. J. Cziczo (2011), Ice nucleation and droplet formation by bare and coated soot particles, *J. Geophys. Res.*, *116*, D17203, doi:10.1029/2011JD015999.

1. Introduction

[2] The interactions between clouds and aerosol particles, and their ability to indirectly influence climate, remains poorly understood [*Forster et al.*, 2007]. This is especially true for ice cloud interactions with aerosol particles. Ice crystals develop from the nucleation and growth of water ice on preexisting aerosol particles [*Pruppacher and Klett*, 1997]. Understanding the connections between the chemical composition of the aerosol particles and their propensity to nucleate ice under various meteorological conditions remains a key requirement for developing a predictive capability to elucidate the impact of ice clouds on climate and the potential for human influence on this process [*Lohmann*, 2002].

[3] The formation of an ice crystal via primary nucleation occurs via two pathways: homogeneous and heterogeneous ice nucleation. Homogeneous ice nucleation is the spontaneous freezing of an aqueous solution droplet, and has been found experimentally to require temperatures cooler than 237 K for atmospherically relevant particle sizes [*Pruppacher and Klett*, 1997]. Heterogeneous ice nucleation involves an insoluble or partially water-soluble ice nucleus (IN) that facilitates ice formation at lower supersaturations and/or warmer temperatures than the homogeneous freezing threshold. While homogeneous ice nucleation can be parameterized by a function of water activity [*Koop et al.*, 2000], the dominant mechanisms of heterogeneous ice nucleation under atmospheric conditions and their dependence on the chemical composition of the ice nucleus remain unclear. Heterogeneous ice nucleation mechanisms include deposition ice nucleation, condensation freezing, immersion freezing, and contact freezing [*Pruppacher and Klett*, 1997]. In the deposition mode, water vapor at temperatures less than 0°C is adsorbed directly onto the surface of the IN to form ice. In condensation freezing, an aerosol particle at a temperature less than 0°C activates to form a liquid droplet which then freezes during condensation. Immersion freezing involves an IN immersed into a droplet; freezing occurs when the temperature of the droplet cools sufficiently below 0°C. An IN acting in the contact mode will

[1]Department of Atmospheric Sciences, University of Washington, Seattle, Washington, USA.
[2]Pacific Northwest National Laboratory, Richland, Washington, USA.
[3]Now at Department of Earth, Atmospheric, and Planetary Sciences, Massachusetts Institute of Technology, Cambridge, Massachusetts, USA.

0148-0227/11/2011JD015999

initiate the ice phase at the moment of contact with a supercooled droplet [*Cantrell and Heymsfield*, 2005; *Pruppacher and Klett*, 1997].

[4] Black carbon, or soot, is commonly found in tropospheric aerosol particles [*Murphy et al.*, 2006]. Soot particles are emitted directly into the atmosphere from combustion processes such as agricultural burning, forest fires, domestic heating and cooking, and transportation. Aircraft traffic is a source of soot particles in the middle and upper troposphere, where temperatures are cooler and ice particles may be more likely to nucleate. Ice core measurements also suggest an increase in soot particle concentrations since preindustrial times due to human activity [*Seinfeld and Pandis*, 2006]. Furthermore, while freshly emitted soot particles are highly hydrophobic, any atmospheric aging associated with condensation of trace gases and oxidation may alter the hygroscopic properties of soot [*Khalizov et al.*, 2009; *Maria et al.*, 2004; *Weingartner et al.*, 1997; *Zhang et al.*, 2008]. Previous field studies involving single-particle analysis provide clear evidence of atmospheric aging and coating of soot particles [*Ebert et al.*, 2010; *Richardson et al.*, 2007]. Similar studies of ice particle residues show an enrichment of soot particles relative to interstitial aerosol [*Cozic et al.*, 2008; *Ebert et al.*, 2010]; whether these data represent scavenging of soot by ice crystals or soot acting as an IN remains in question. Organic-rich particles have been shown to require much higher supersaturations in order to nucleate ice [*Cziczo et al.*, 2004; *DeMott et al.*, 2003]. Previous studies have also shown micrometer sized glutaric acid, maleic acid, and long-chain organic particles to nucleate ice heterogeneously at temperatures ranging from 190 to 240 K [*Baustian et al.*, 2010; *Beaver et al.*, 2006; *Shilling et al.*, 2006]. Yet, due to the relatively low concentrations of heterogeneous IN, as well as the increase in anthropogenic emissions of soot particles, it is important to understand the effects of mixing state, size, and chemical composition of a soot particle on its ability to act as an IN [*Kärcher et al.*, 2007].

[5] Laboratory studies to date have produced mixed results regarding the ability of soot particles to act as IN. Previous laboratory studies on the ice nucleation of soot particles at temperatures representative of heterogeneous ice nucleation have differed in their methods of particle generation, from acetylene combustion [*DeMott*, 1990], kerosene combustion [*Diehl and Mitra*, 1998], benzene and toluene combustion as well as thermal decomposition of benzene [*Gorbunov et al.*, 2001], and N-hexane diffusion flame and commercial carbon black [*Dymarska et al.*, 2006]. These studies mainly focused on heterogeneous ice nucleation at or above water saturation, with the exception of *Dymarska et al.* [2006], which focused on deposition ice nucleation occurring below water saturation for a variety of soot types. That study found that deposition ice nucleation was not important for soot particles at temperatures above 243 K and below water saturation. Ozone exposure also did not alter the ice nucleation activity of the soot particles. Above water saturation, it is suggested that immersion or condensation freezing may be important, yet the contribution to total IN concentrations of soot particles acting as immersion or as condensation freezing IN in the atmosphere is unknown. *DeMott* [1990] suggested that because water supersaturations may only be sustained for transient periods in cirrus clouds, soot particles acting as immersion IN may not have a large impact of the total ice content of cirrus clouds. It is noteworthy that some previous studies contradict the majority of results and suggest that soot particles can act as IN at temperatures as warm as 253 K and at low supersaturations with respect to ice, depending on the level of oxidizing groups on the soot particle surface [*Diehl and Mitra*, 1998; *Gorbunov et al.*, 2001].

[6] Soot studies at temperatures cooler than 237 K have considered soot particles of various chemical compositions. A common theme to these results has been the importance of the particle's mixing state [*DeMott et al.*, 1999; *Möhler et al.*, 2005a] and hygroscopic properties [*Koehler et al.*, 2009; *Möhler et al.*, 2005b]. *Koehler et al.* [2009] studied a suite of soot particles at temperatures colder than 233 K, ranging from hydrophobic to hydrophilic, and found that heterogeneous ice nucleation was favored on oxidized hydrophilic soot, with a maximum of 1% of soot particles forming ice at 221.5 K. Further, *Möhler et al.* [2005b] suggested that a higher organic carbon content suppressed ice nucleation on soot particles at 207 K, which suggests that the increase of organic carbon added to the hydrophobicity of the soot particle. An alternate explanation regards the formation of a highly viscous or amorphous coating around the soot particles, which may impede ice nucleation [*Murray*, 2008; *Zobrist et al.*, 2008]. Ice nucleation for the soot particles with a higher organic carbon content occurred at approximately the homogeneous freezing threshold, whereas soot particles with a lower organic carbon content nucleated ice slightly below the homogeneous freezing threshold. A recent study by *Crawford et al.* [2011] found that at a temperature of 226.6 K heterogeneous ice nucleation was most efficient for uncoated propane soot of low organic carbon content (approximately 5% organic carbon content). Increasing the organic carbon content to approximately 30% and 70% significantly lowered the ice nucleation efficiency of the propane soot; water saturation was required for freezing to occur.

[7] In the following study we generated coated and uncoated soot particles of variable size and composition to study their ice formation at temperatures relevant to heterogeneous and homogeneous ice nucleation, as well as their associated hygroscopicity. Three different coating materials were used with a range of solubilities in order to investigate the possible effect on ice nucleation. The results were interpreted in terms of onset ice nucleation, comparison to a known mineral dust particle that acts as an IN, and particle hygroscopicity. In this way we assess the connection between the chemical and physical properties of laboratory-generated soot particles with their respective ice nucleation properties in an attempt to further our understanding of the contribution of soot particles to the global IN concentration.

2. Methods

2.1. Particle Generation and Characterization

[8] The experimental setup is shown in Figure 1. Soot particles were generated in a diffusion flame with propane as fuel using a miniCAST Real Soot Generator (Jing Ltd.). To generate soot particles with low organic content the flame was operated under lean conditions, with the flow rates of propane fuel, oxidation air, quench gas (N_2), and dilution air of 0.06, 1.55, 7.5, and 20 L min^{-1}, respectively. Soot particles were collected for sampling in a 100 L Teflon bag

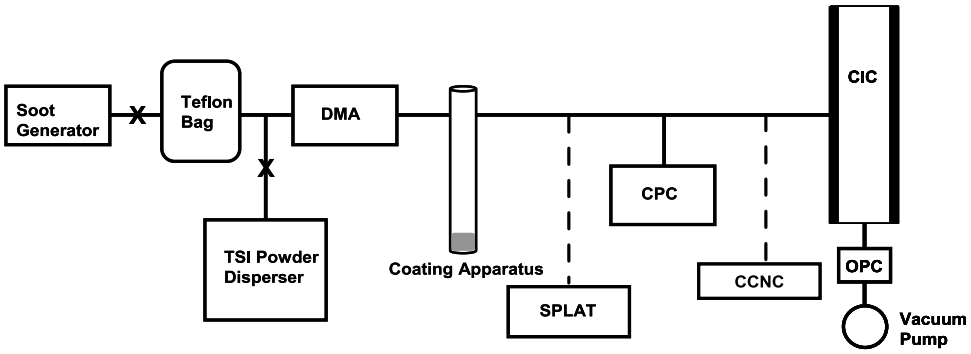

Figure 1. Schematic view of the experimental setup. Particles were periodically sent to a single-particle laser ablation time-of-flight mass spectrometer (SPLAT) for characterization, as indicated by a dashed line. Ice nucleation experiments utilized the compact ice chamber (CIC); in the case of droplet activation experiments, the CIC in the experimental setup was replaced by a cloud condensation nuclei counter (CCNC), as indicated by a second dashed line. The soot generator was not operating continuously; particles were sampled and size-selected from a Teflon bag. In the case of the kaolinite experiments, particles were generated with a TSI powder disperser before sizing.

and their mobility diameter (d_m) size distributions were measured using a scanning mobility particle sizer (SMPS) (TSI 3936). IN and cloud condensation nuclei (CCN) experiments were conducted on 100, 200, and 400 nm (d_m) particles size-classified by a differential mobility analyzer (DMA, TSI 3080) and counted by a condensation particle counter (CPC, TSI 3010).

[9] Coated particles were generated by passing the size-selected soot particles at a flow rate of 0.3 L min^{-1} through a heated temperature-controlled reservoir containing the coating organic substance, which included either malic acid, adipic acid, or oleic acid. Temperatures during the coating process were adjusted, for each organic material, to achieve the desired coating thicknesses, and kept below the temperature at which homogenous nucleation of the coating acid takes place. The phase of the coating material was not directly determined by these techniques. At the temperature and relative humidity conditions of the ice nucleation experiments supercooled aqueous solutions as well as crystalline solids are possible [*Hearn and Smith*, 2005].

[10] The vacuum aerodynamic diameter (d_{va}), chemical composition, and effective density of DMA-classified coated and uncoated particles were characterized using a single-particle laser ablation time-of-flight mass spectrometer, SPLAT II, that has been described in detail elsewhere [*Zelenyuk and Imre*, 2005, 2009]. Here we provide a brief description only. Particles are drawn into the instrument through an aerodynamic lens inlet used to transport the particles from the ambient air into the vacuum system with high efficiencies. The aerodynamic lens forms a low divergence beam and imparts on each particle a velocity that is a function of the particle d_{va}. Individual particles are detected by light scattering at two optical detection stages located 10.5 cm apart. The particle time of flight (PTOF) between the two stages is used to calculate particle velocity and determine its d_{va} with 0.5% precision. The particle detection event and the PTOF are then used to generate triggers to fire the infrared CO_2 and ultraviolet excimer lasers for particle evaporation and ionization, respectively. Individual particle chemical compositions are determined from the acquired mass spectra using an angular reflectron time-of-flight mass spectrometer. Particle density or effective density, and fractal dimension are determined based on the measurements of d_{va} distribution of DMA size classified particles [*Zelenyuk and Imre*, 2009].

[11] To obtain thin coating layers, coatings reservoir temperatures were set to assure that the particle mobility diameters of coated and uncoated soot particles remain nearly the same, as illustrated in Figure 2a, while their vacuum aerodynamic diameters (d_{va}) increase by approximately 10 nm to 20 nm (Figure 2b). Once this condition was reached with one size of the soot core, the process was repeated on soot particles with different mobility diameters and for each d_m the d_{va} distributions were measured. In addition, the presence of thin organic acid coating was confirmed using the individual particle mass spectra, as demonstrated for adipic acid coating in Figure 2c. Finally, the data for each condition were used to obtain the relationship between the d_m and the d_{va} to assure that coated particles maintain the fractal structure of the soot particles (Figure 2d). When thick coatings were generated, they resulted in apparent changes in d_m (Figure 2a), larger changes in particle d_{va} (Figure 2b, approximately 80 nm to 100 nm), and increased fractal dimension of the coated particles that corresponds to more compact particles (not shown). We assume from the resulting size distributions and mass spectra that thin coatings are partial coatings, and thick coatings are more complete coatings, although it must be noted that partially or completely bare soot particles cannot be completely precluded even in conditions defined as thickly coated.

[12] Previous studies have speculated that the oxidation of soot by ozone will enhance soot's IN activity [*Gorbunov et al.*, 2001]. In addition to the soot particles coated with malic and adipic acids, we also investigated the IN and CCN activities of soot particles coated with oleic acid as well as the coated and bare soot particles aged in the presence of ozone.

[13] Kaolinite particles were employed to provide a comparison to previous studies and to the soot particle results. As a component of mineral dust, kaolinite has been a focus of many past ice nucleation studies and its ability to act as an IN has been extensively documented previously [*Eastwood et al.*, 2008; *Kanji and Abbatt*, 2006; *Murray et al.*, 2010; *Welti et al.*, 2009]. Kaolinite particles were generated via a

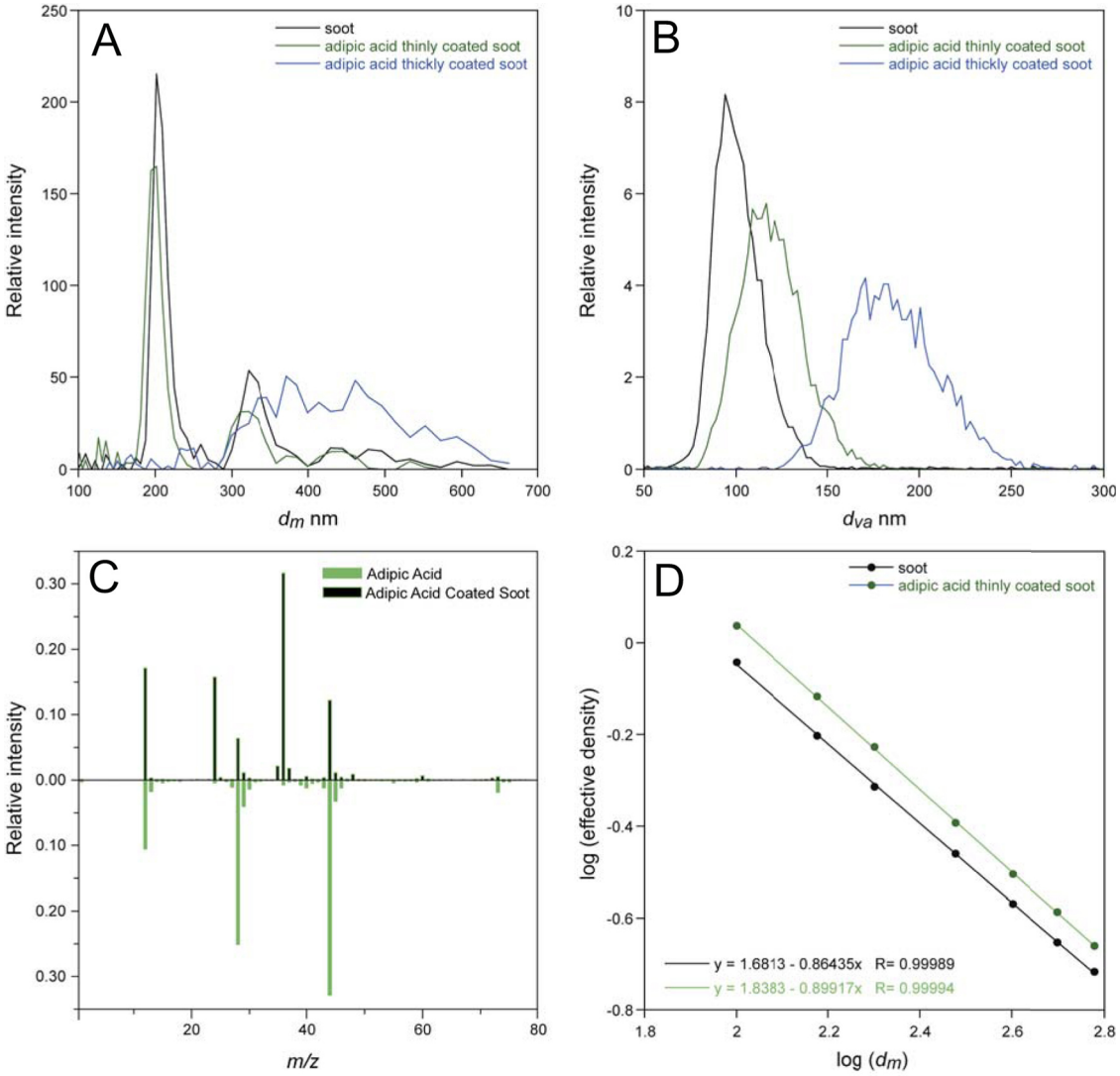

Figure 2. (a) Mobility diameter (d_m) as measured by the differential mobility analyzer for bare soot (black line) and for thin and thick coatings of adipic acid (green and blue lines, respectively). (b) Vacuum aerodynamic diameter (d_{va}) as measured by SPLAT for bare soot (black line) and for thin and thick coatings of adipic acid (green and blue lines, respectively). (c) Mass spectra for adipic acid (green, inverted spectrum) and for soot thinly coated with adipic acid (black). (d) Fractal dimension of soot (black line) and of soot thinly coated with adipic acid (green line).

small-scale powder disperser (TSI 3433) and subsequently size-selected with a DMA.

2.2. Ice Nucleation

[14] The ice nucleation technique utilized has been described in the literature previously [*Stetzer et al.*, 2008]. The Pacific Northwest National Laboratory (PNNL) compact ice chamber (CIC) is a continuous flow diffusion chamber consisting of two flat, parallel aluminum plates that are cooled and covered with a layer of ice. The two plates are cooled to different temperatures below the bulk freezing point of water, generating a linear gradient in water vapor partial pressure and temperature between the two plates. Because of the nonlinear relationship between saturation vapor pressure and temperature, supersaturation with respect to ice is generated along the center of the column. Generated particles flow through the center lamina of the chamber "trapped" by two identical particle-free sheath flows that pass along the plate. This serves two purposes. First, particles do not interact with the walls. Second, particles are confined to the specific temperature and relative humidity at the center of the lamina. Ice particle formation is detected by an optical particle counter (OPC) at the chamber exit. The OPC (CLiMET, model CI-3100) has been modified to produce the particle size distribution (a function of the sheath to sample flow ratio and the specific experimental conditions). This is done by extracting the raw counts from the OPC and binning them according to size using an in-house built multiple channel analyzer board. The size distribution is later calibrated using the standard available sizes. The OPC measured particles from

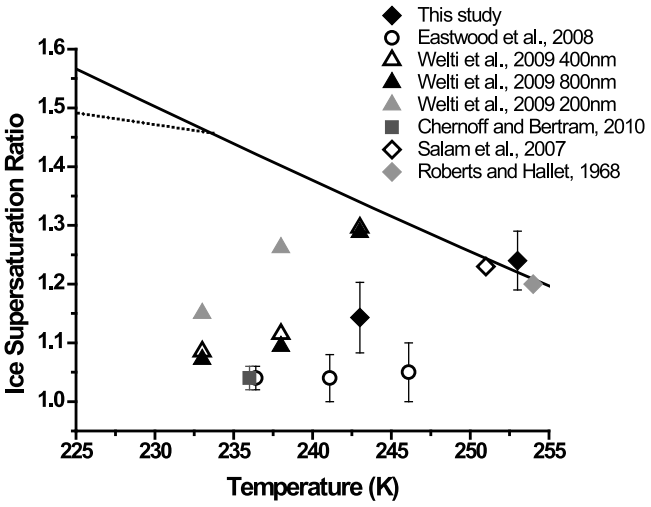

Figure 3. Onset RH_i conditions of ice formation for kaolinite particles for a variety of studies at various temperatures. Results from this study are shown by the filled black diamonds. Kaolinite particles were size-selected at 300 nm. Solid black line indicates water saturation; dotted black line indicates the homogeneous freezing threshold for a 200 nm particle [*Koop et al.*, 2000].

700 nm to 10 μm diameter but does not have phase discrimination capability.

[15] The chamber is able to reach temperatures as low as 233 K, and has a fixed residence time of approximately 12 s and a flow rate of approximately 10 litres min^{-1} such that nucleated ice crystals are able to grow to sizes of several micrometers. In each experiment the average temperature of the chamber was held constant while the relative humidity was slowly increased from subsaturated to supersaturated conditions with respect to water. Under no conditions were ice crystal concentrations large enough to impact their growth rates due to water vapor depletion. We investigated both heterogeneous and homogeneous ice nucleation of our system of particles at temperatures of 253, 243, and 233 K.

[16] The ice chamber terminates in an evaporation section, maintained at ice saturated conditions. The purpose of this section is to evaporate liquid droplets which do form while maintaining the size of nucleated ice crystals, thereby allowing an indirect means of differentiating phase. The length, and therefore residence time, of this section "sets" the supersaturation with respect to water (i.e., the droplet size which can be evaporated) that can be investigated. A threshold size is arbitrarily set to differentiate aerosol and droplet from ice crystals in the OPC. For these experiments this size was set at 2.5 μm diameter. The point at which droplets exceed this threshold size is determined by the aerosol size and residence time, and the operating temperature and relative humidity conditions within the chamber. The chamber conditions that lead to droplets above the threshold size are discussed more completely in later sections but, briefly, conditions just over water saturation were observed to lead to droplet formation, and we were therefore not able to investigate significantly beyond this range. In the future we will investigate the effect of a lengthened evaporation section on the conditions which allow for droplet breakthrough.

[17] At saturation ratios below droplet breakthrough the activated fraction of ice was determined from the ratio of particles exiting the chamber, as measured by the OPC, to the number of entering particles measured by the CPC. The OPC detects and measures particles larger than 700 nm. The OPC was used to differentiate ice from unactivated particles at a size of 2.5 μm diameter. That is to say, while particles larger than 700 nm were detected, these were not counted as activated until reaching a size of 2.5 μm. Ice formation onset is reported as the relative humidity with respect to ice (RH_i) at which 1% of particles grow beyond 2.5 μm. With a particle-free flow in the CIC, the OPC shows background counts due to instrument noise and occasional frost crystals that correspond to a fraction of particles used in these experiments ranging between 0.01–0.1% (approximately 10 per liter at the experimental particle concentration). This background was subtracted from the data; this sets the ice nucleation detection threshold and the remaining data shows nucleation occurring above this detection limit.

[18] Two further experimental limitations are noteworthy. First, losses in the CIC were measured by placing identical CPCs at the top and bottom of the chamber. Losses are variable, depending on flow and particle properties, and on the order of 20% (±10%) of the entering particles, based on 200 nm ammonium sulfate particles. Activation is therefore not expected to attain fully 100% of input particles. Second, as discussed in the previous section, above water saturation, liquid droplets are able to grow larger than the OPC size threshold. Because the OPC measurement at the bottom of the chamber cannot distinguish phase, at this supersaturation value we cannot differentiate between the formation of liquid droplets and the activation of ice particles. Note that this does not affect observation of deposition nucleation which predominantly occurs below water saturation, but it limits the relative humidity (supersaturation) range over which immersion or condensation freezing can be observed. Data points occurring above this droplet breakthrough supersaturation threshold are not considered representative of heterogeneous ice nucleation, although we cannot preclude heterogeneous nucleation also occurring in parallel to, or after, droplet formation.

2.3. Droplet Activation

[19] In addition to ice nucleation, the droplet nucleation ability of the particle systems was also studied as a means to infer hygroscopicity. The cloud condensation nuclei counter (CCNC) manufactured by Droplet Measurement Technologies is a continuous flow streamwise thermal gradient open cylinder CCN counter that has been described in detail in previous literature [*Lance et al.*, 2006; *Roberts and Nenes*, 2005]. Briefly, flow into the CCNC is split into an aerosol and sheath flow; the sheath flow is filtered, humidified, and heated, and acts to limit the main aerosol flow to the center of the CCNC column in the same manner as done in the CIC. A positive temperature gradient is then applied to the continuously wetted column in the direction of the flow analogous to the cross-flow gradient in the CIC. Due to the contrast in diffusion rates between water and heat, supersaturation with respect to water vapor is generated along the center of the column. Particles will grow to droplets when the supersaturation in the column is equal to the critical supersaturation for the given particle and the value

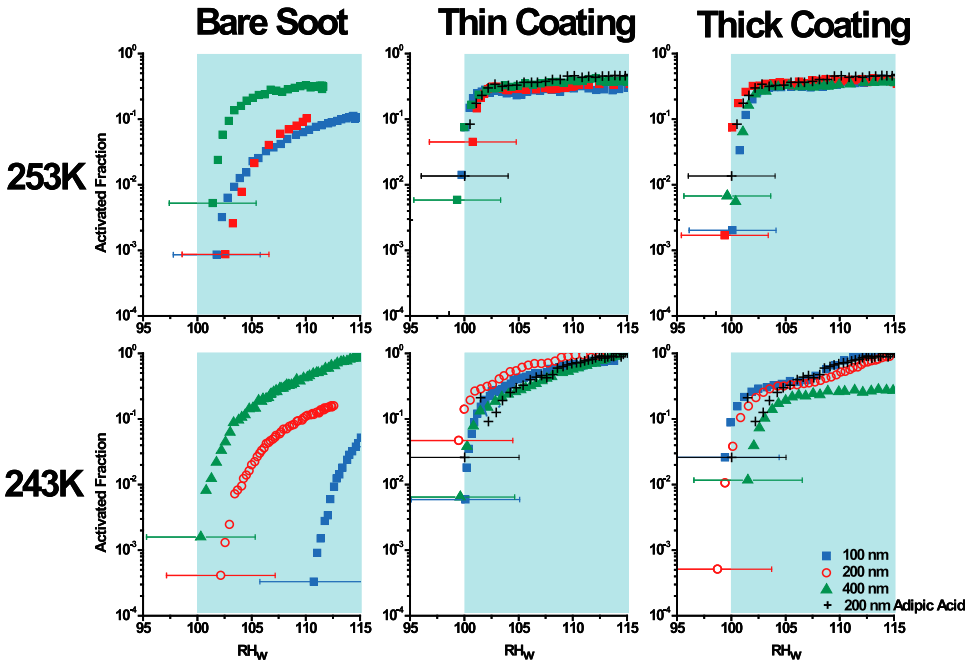

Figure 4. Activated fraction of particles as a function of relative humidity with respect to water (RH_w) and size. Plots show the results of experiments in which the CIC temperature was held constant at (top) 253 K and (bottom) 243 K while the RH_w was gradually increased. All six plots show the activated fraction of bare soot particles, soot particles thinly coated by adipic acid, and soot particles thickly coated by adipic acid. Color scheme is the same for each plot: 100 nm core soot particles (blue squares), 200 nm core soot particles (open red circles), and 400 nm core soot particles (green triangles). Black plus signs show the 200 nm adipic acid particles. The droplet breakthrough region, the lower limit of the zone in which the CIC cannot differentiate between ice and droplet particles, is represented by the blue shading. No ice nucleation is observed under conditions outside the droplet breakthrough region. For clarity, error bars are shown for just one data point; error bars apply to all data points. Note that soot coated with adipic acid behaved similarly to soot coated with oleic acid and malic acid.

at which 50% of the particles activate as droplets is normally reported. Droplets growing to sizes greater than 1 μm are then detected by an OPC. The CCNC was calibrated with selected ammonium sulfate particles generated by atomizing a 0.1 M aqueous solution of ammonium sulfate.

[20] Water vapor supersaturation in the column was varied from 0.1% to 1.0% at room temperature (~295 K). The activated fraction is calculated and reported as the number of activated droplets relative to the total number of particles entering the CCNC, as measured by a CPC.

3. Results and Discussion

3.1. Ice Nucleation of Kaolinite Particles

[21] For comparison and validation purposes, the ice nucleation properties of size-selected kaolinite particles were investigated at similar temperature conditions to the experiments involving size-selected soot particles. Results for ice nucleation onsets for 253 K and 243 K are shown in Figure 3. The onset relative humidity for 1% ice formation utilizing the PNNL CIC is consistent with the broad range of previous measurements that utilized a range of instruments and techniques to generate kaolinite particles and assess their ice nucleation activity [*Chernoff and Bertram*, 2010; *Dymarska et al.*, 2006; *Eastwood et al.*, 2008; *Roberts and Hallett*, 1968; *Salam et al.*, 2007; *Welti et al.*, 2009].

3.2. Activated Fractions of Ice Above the Homogeneous Freezing Temperature

[22] Each experiment at a constant temperature was conducted to yield an activated number concentration as a function of relative humidity. For conditions below water droplet breakthrough, this was interpreted as an ice particle number concentration which was then converted to an activated fraction of ice by comparison to the number of particles entering the ice chamber above the instrumental detection limit. An example of these data at 253 and 243 K (above the homogeneous freezing threshold) is shown in Figure 4. Figure 4 shows the activated fractions as a function of relative humidity for three sizes of soot particles before and after both thin and thick coatings of adipic acid were applied, as well as pure adipic acid particles.

[23] The droplet breakthrough region, indicated in blue, is representative of the relative humidity at and above which unfrozen water droplets would grow to sizes detectable by the OPC preventing quantification of ice nucleation. Data points shown occurring within the experimental error of the droplet breakthrough threshold cannot be precluded from being due to droplet formation. Note that we only show data points where there was a clear signal above background; data were acquired at lower RH_w values than shown by the data points shown in Figure 4 but in all cases were below the background. The results in Figure 4 indicate that

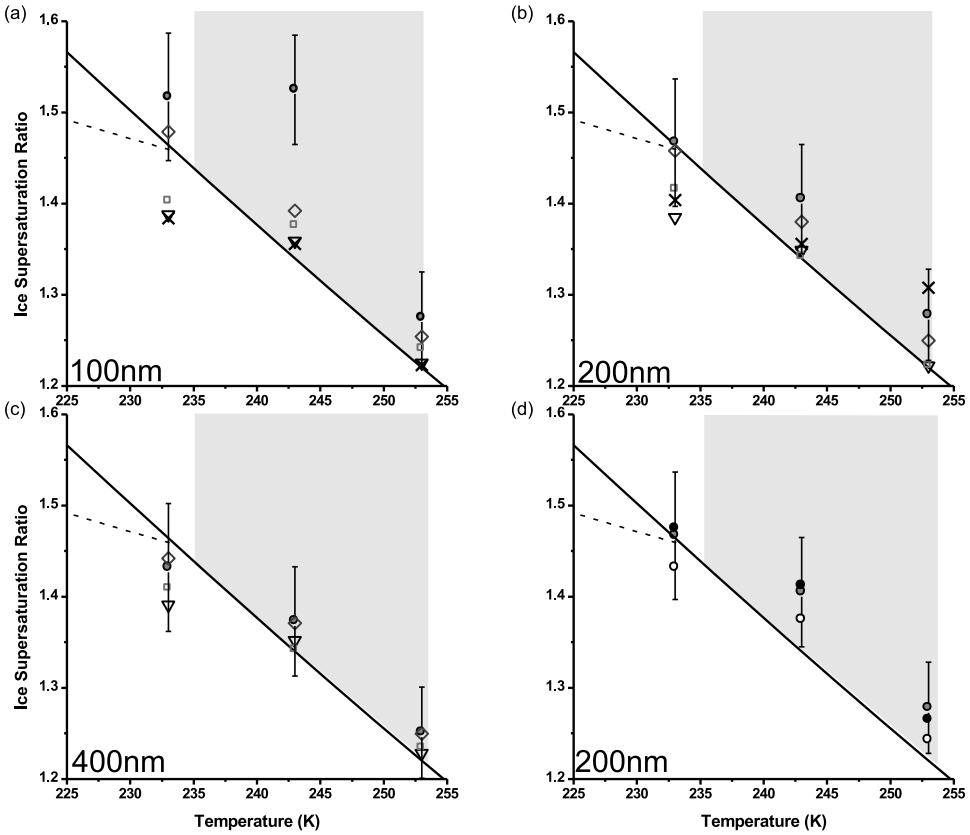

Figure 5. Onset conditions for the detectable activation (ice or droplet formation) of 1% of bare soot particles (shaded circles), soot thinly coated with adipic acid (triangles), pure adipic acid (crosses), soot thinly coated with malic acid (squares), and soot thinly coated with oleic acid (diamonds) nucleating as a function of RHi, temperature, and size. Onset conditions are shown for (a) 100 nm core soot particles, (b) 200 nm core soot particles, and (c) 400 nm core soot particles. Symbols are the same for all plots. (d) Onset conditions for 1% nucleation of 200 nm bare soot particles (gray circles), 200 nm soot exposed to ozone (open circles), and 200 nm soot thinly coated with oleic acid and exposed to ozone (filled circles). Solid black line indicates water saturation; dashed black line indicates the homogeneous freezing threshold for 200 nm particles [*Koop et al.*, 2000]. For clarity, error bars are shown on bare soot particles only; the error bars shown on bare soot particles apply to each data point. Uncertainties in the ice supersaturation ratios were calculated from the uncertainties in the CIC temperature measurements. The gray-shaded region represents the droplet breakthrough. Note that ice nucleation is not observed outside of homogeneous freezing conditions.

heterogeneous ice nucleation does not occur above the instrument background before the formation of droplets, at which point we can no longer assess if and when freezing may have occurred. The morphology of the activation curves supports the conclusion that droplet and not ice nucleation is occurring in these experiments. Ice nucleation, had it occurred, would result in the formation of a small number of large particles followed by nearly all particles forming droplets [*Petters et al.*, 2009]. No "shoulder" corresponding with ice nucleation was evident in any of the experiments. Instead, only a constant increase consistent with drop formation was observed. Furthermore, experiments were conducted with pure adipic acid aerosols which are known not to freeze heterogeneously. These experiments indicated a similar increase in the formation of large particles which cannot be attributed to ice formation. While we cannot preclude heterogeneous ice nucleation occurring below the detection limit we can set the upper limit for a maximum contribution of 0.01% of soot particles acting as heterogeneous IN before the onset of droplet formation.

[24] The droplet activated fractions and breakthrough of bare soot particles do show a size effect at both temperatures, with the largest sized particles showing droplet nucleation at relatively lower relative humidity values. After coating, this size dependence collapsed, and coated particles of all sizes behaved similarly. This may be due to the role coatings play in water uptake, which overrides any competing size effect from the core soot particles.

3.3. Uncoated Soot Particles

[25] The onset of ice formation is determined as the relative humidity value at which 1% of particles nucleated ice, at the given temperature. The gray circles in Figures 5a, 5b, and 5c show the relative humidity with respect to ice at

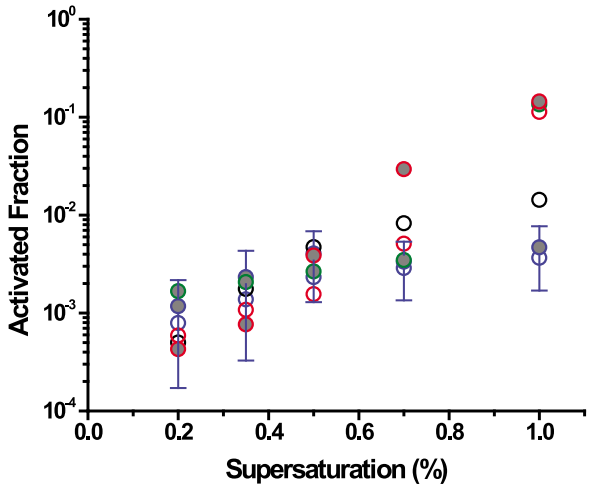

Figure 6. The cloud condensation nuclei results for a variety of particles as a function of activated fraction and supersaturation with respect to water. Open circles represent 100 nm soot (blue), 100 nm soot coated with oleic acid (black), and 100 nm soot coated with oleic acid and exposed to ozone. Gray-filled circles represent 400 nm soot (blue), 400 nm soot coated with malic acid (green), and 400 nm soot coated with oleic acid and exposed to ozone (red). For clarity, the error bars are shown only on the 400 nm soot; the error bars correspond to all particles studied.

which 1% of particles grew large enough to be detectable by the OPC, as a function of temperature and soot particle size. The start of the droplet breakthrough region is indicated by the blue shading. As described in section 3.2, ice nucleation was not observed before droplet formation at temperatures warmer than required for homogeneous freezing, after which we cannot distinguish between droplets and ice particles.

[26] Similarly, we did not observe ice nucleation before the threshold relative humidity for homogeneous nucleation at lower temperatures, with one exception. Soot particles sized at 400 nm nucleated ice below the threshold for homogeneous freezing (Figure 5, dashed black line) [*Koop et al.*, 2000] at 233 K. However, the uncertainty in the relative humidity measurements (shown as the error bars in Figure 5) at 233 K is sufficiently large that we cannot rule out the occurrence of homogeneous freezing alone being responsible for all ice formation.

3.4. Soot Coated With Organic Acids and Exposed to Ozone

[27] Soot particles were coated with malic, adipic, and oleic acid, chosen based on their respective solubility properties and abundance in the atmosphere [*Broekhuizen et al.*, 2004; *Carvalho et al.*, 2003; *Claeys et al.*, 2010; *Cruz and Pandis*, 1997; *Hings et al.*, 2008; *Hsieh et al.*, 2007; *Kawamura et al.*, 1996; *Rissman et al.*, 2007; *Saxena and Hildemann*, 1996; *Sempére and Kawamura*, 1994]. In the coating studies presented in this paper, thin and thick coatings of malic and adipic acid and a thin coating of oleic acid were deposited onto the soot particle "cores."

[28] Results for the ice saturation ratios at which 1% droplet or ice formation occurred at the studied temperatures as a function of size are included in Figure 5. Similar to bare soot particles described in the previous section, the resulting onsets of ice formation show that ice formation did not occur below water saturation for the coated particles of all sizes at temperatures warmer than 233 K. Further, given the detection limits of the CIC, we did not see evidence for heterogeneous ice nucleation before the formation of droplets. The addition of adipic acid and malic acid coatings did not significantly alter this behavior, and most likely aided in droplet formation at supersaturations greater than water saturation. The addition of a thin insoluble coating, oleic acid, also did not change the ice nucleation of uncoated soot particles. At 233 K, all sizes of soot particles coated with both malic acid and adipic acid, and 400 nm particles coated with oleic acid nucleated ice below water saturation and the homogeneous freezing threshold, while 100 nm and 200 nm particles coated with oleic acid nucleated ice at or above water saturation. Given uncertainty in the relative humidity measurements at 233 K, it is possible that these particles froze homogeneously at this temperature.

[29] In addition to studying ice nucleation of coated soot particles, we also generated pure adipic acid particles and pure oleic acid particles and studied their ice nucleation activity at the same experimental conditions as outlined previously. These particle types would not be expected to nucleate ice heterogeneously and, indeed, all sizes of adipic acid particles behaved similarly to all sizes of soot coated with adipic acid (Figure 5). All sizes of pure oleic acid nucleated ice at higher supersaturations than soot coated with oleic acid. These results support the conclusion that soot and coated soot particles did not nucleate ice before the droplet breakthrough regime.

[30] We also exposed both bare soot particles and soot coated with oleic acid to 2 ppm of ozone for 1 h, equivalent to approximately 3.5 days of atmospheric aging. The droplet/ice nucleation onsets are shown in Figure 5 for 200 nm core soot particles (bottom right). Ozone exposure for both particle types did not significantly alter the ice nucleation behavior. This result is similar to that of *Dymarska et al.* [2006], in which oxidation of soot particles by ozone did not have a significant effect on the ice nucleation behavior of the soot particles at temperatures greater than 240 K.

3.5. CCN Activation of Various Soot Particle Types

[31] Droplet activation studies of soot are shown in Figure 6, in terms of the activated fraction of droplets as a function of water supersaturation in the CCNC. Uncoated soot particles were hydrophobic, as they did not activate as droplets at water supersaturations up to 1%.

[32] Soot coated with oleic acid did not activate as droplets even at water supersaturations as large as 1%. Soot coated with malic and oleic acid and exposed to ozone both achieved an activated fraction of approximately 10% at a water supersaturation of 1%. In general, the soot particles generated in this study were hydrophobic, and applying a coating of malic acid or exposing oleic acid coated soot to ozone aided in activating only a small percentage of droplets at the highest water supersaturations investigated. These results agree with the work of *Popovicheva et al.* [2008, 2009, 2011] in that soot particles with low oxygen content were found to be hydrophobic and also that the properties of

the organic component coverage on the surface of the soot particle determined the water uptake.

4. Atmospheric Implications

[33] Given the lifetime and size distribution of soot particles emitted into the atmosphere, particles from aircraft and incomplete combustion emissions become mixed with ambient species [*Riemer et al.*, 2004; *Slowik et al.*, 2007; *Zhang et al.*, 2008]. Thus, we can assume that a fraction of atmospheric soot particles have some soluble material associated with them, either on the surface or within the bulk of the particle. Our experiments show that a coating of a soluble organic acid on the types of hydrophobic soot particles used in this study does not significantly increase the efficiency of ice nucleation, as compared to the uncoated soot particle. Specifically, our experiments show that at 253 K and 243 K, heterogeneous ice nucleation does not occur below water saturation for all particle sizes studied. While we cannot preclude heterogeneous ice nucleation occurring below the detection limit, we can set an upper limit for a maximum activated fraction of 10^{-4} of soot particles acting as heterogeneous IN. Our results also show that the addition of soluble and moderately soluble organic species to the surface of the soot particles did not significantly affect the soot particle's ability to nucleate ice heterogeneously or homogeneously. At 233 K, soot coated with malic acid and adipic acid nucleated ice slightly lower than soot particles and soot coated with oleic acid. However, all ice nucleation occurred within the experimental uncertainty of the homogeneous freezing saturation at this temperature, and we therefore cannot confirm that any heterogeneous nucleation took place at this temperature. Ozonolysis of the soot particles and the oleic acid coated soot particles also did not significantly change the ice nucleation of the uncoated soot particles.

[34] Our results are in agreement with those of *Dymarska et al.* [2006], *Möhler et al.* [2005a, 2005b], and *DeMott et al.* [1999] in that freshly emitted soot as well as atmospherically aged soot particles are unlikely to act as ice nuclei in the deposition freezing mode. *Dymarska et al.* [2006] studied a range of soot particles at temperatures between 243 and 258 K, and were unable to confirm heterogeneous ice nucleation once liquid water was present. Our experiments confirm those results and also extend the temperature range and the particle types investigated. Our results at 233 K also confirms the results of *DeMott et al.* [1999] and *Möhler et al.* [2005a, 2005b] in that the addition of adipic acid and malic acid coatings on the soot particles lowered the threshold ice supersaturation ratios necessary for 1% ice nucleation below the homogeneous freezing line, yet not sufficiently enough to rule out the occurrence of homogeneous ice nucleation within our experimental uncertainty. Further, *Koehler et al.* [2009] did not observe the occurrence of deposition ice nucleation at 233 K. In contrast, *Gorbunov et al.* [2001] suggested that at 253 K and at low supersaturation ratios with respect to ice (1.1–1.2), oxidized soot particles are a very important source of ice nuclei and could account for 10% of the typically observed IN concentrations. Additionally, *Diehl and Mitra* [1998] showed up to 70% of large, but unquantified, soot particles from a kerosene burner froze at temperatures between 245 K and 255 K. In contrast to both *Gorbunov et al.* [2001] and *Diehl and Mitra* [1998] our experiments show a lack of significant ice nucleation outside of the homogeneous freezing regime and that there is not a significant difference in the ice nucleation behavior of hydrophobic soot particles and soot particles coated with a soluble material. Further, we did not observe any heterogeneous ice nucleation onsets at greater than 10^{-4} fractions active at 253 K.

[35] In order to understand the magnitude of climate forcing due to the presence of IN at a range of atmospheric conditions, cloud models have used simplified parameterizations or relationships between specific particle types and their ability to act as an IN developed in the laboratory and atmosphere [*Fletcher*, 1958; *Kärcher*, 1996; *Kärcher and Lohmann*, 2003; *Lohmann*, 2002; *Lohmann and Diehl*, 2006; *Meyers et al.*, 1992; *Phillips et al.*, 2008]. A few studies have also considered soot particles to be an IN on the same order as kaolinite [*Aquila et al.*, 2010]. The study presented in this paper clearly shows that at temperatures greater than 233 K, soot particles are unlikely to act as heterogeneous IN in the deposition freezing regime. Our results extend only slightly into conditions supersaturated with respect to water. This result is particularly striking when compared to experiments on kaolinite which effectively nucleated ice at saturations between 1.1 and 1.2 at 243 K. These results strongly suggest that typical atmospheric aging processes are unlikely to improve the ice nucleating ability of soot particles and that soot particles are unable to act as IN at similar conditions and magnitudes as "good" IN, such as mineral dust components. To the extent that soot particles are involved in atmospheric ice formation at temperatures ranging from 233 K to 253 K, as inferred from some ice residue measurements, we suggest that heterogeneous mechanisms are not involved or require a more exotic component not present in our laboratory generated particles.

5. Summary

[36] In this study we investigated the ice nucleating properties of bare and coated soot particles with a range of organic acids and exposed to ozone at three temperatures. We validated the ability of our experimental setup to detect ice formation and compared our results to previous reports of the ice nucleation properties of size-selected kaolinite particles. Droplet activation studies were also conducted for selected particles. We saw no evidence for heterogeneous ice nucleation above our experimental detection limits at 253 K and 243 K. Above water saturation our results show evidence for the formation of droplets, although we cannot distinguish between droplets and a small amount of freezing occurring after droplet formation. Results indicate that the organic acid coatings aided in water uptake to activate droplets after water saturation was reached. However, the solubility properties of the coating on the soot particle, as well as exposure to ozone, did not significantly affect any ice nucleation behavior of the soot particle. At 233 K, freezing occurred in close correspondence with homogeneous ice nucleation conditions, although we cannot preclude a small amount of heterogeneous freezing of the soot particles coated with adipic acid and malic acid. CCNC

studies indicated soot particles were hydrophobic and did not activate as cloud condensation nuclei at high water supersaturations; soot particles coated with malic acid and soot particles coated with oleic acid and exposed to ozone experienced a slight increase in the activated fraction of droplets at supersaturations greater than 0.7%, consistent with homogenizing droplet activation in the CIC at these conditions.

[37] **Acknowledgments.** The authors wish to thank Olaf Stetzer for many useful discussions and for assistance in construction of the CIC. This work was supported by the Pacific Northwest National Laboratory (PNNL) Aerosol and Climate Initiative and an award from the Department of Energy Science Graduate Fellowship Program (DOE SCGF). The DOE SCGF Program was made possible in part by the American Recovery and Reinvestment Act of 2009. The DOE SCGF program is administered for the DOE by the Oak Ridge Institute for Science and Education (ORISE), which is managed by Oak Ridge Associated Universities (ORAU) under DOE contract DE-AC05-06OR23100. A portion of this work was also sponsored by the U.S. Department of Energy Office of Biological and Environmental Research, the Office of Basic Energy Sciences, and the Division of Chemical Sciences, Geosciences, and Biosciences. The research was performed in the Environmental Molecular Sciences Laboratory, a national scientific user facility sponsored by the DOE's Office of Biological and Environmental Research at PNNL. PNNL is operated for the DOE by Battelle Memorial Institute under DOE contract DE-AC06-76RL0 1830. All opinions expressed in this paper are the authors' and do not necessarily reflect the policies and views of DOE, ORAU, or ORISE.

References

Aquila, V., et al. (2010), MADE-IN: A new aerosol microphysics submodel for global simulation of potential atmospheric ice nuclei, *Geosci. Model Dev. Discuss.*, *3*, 2221–2290, doi:10.5194/gmdd-3-2221-2010.

Baustian, K. J., M. E. Wise, and M. A. Tolbert (2010), Depositional ice nucleation on solid ammonium sulfate and glutaric acid particles, *Atmos. Chem. Phys.*, *10*, 2307–2317, doi:10.5194/acp-10-2307-2010.

Beaver, M. R., M. J. Elrod, R. M. Garland, and M. A. Tolbert (2006), Ice nucleation in sulfuric acid/organic aerosols: Implications for cirrus cloud formation, *Atmos. Chem. Phys.*, *6*, 3231–3242, doi:10.5194/acp-6-3231-2006.

Broekhuizen, K. E., T. Thornberry, P. P. Kumar, and J. P. D. Abbatt (2004), Formation of cloud condensation nuclei by oxidative processing: Unsaturated fatty acids, *J. Geophys. Res.*, *109*, D24206, doi:10.1029/2004JD005298.

Cantrell, W., and A. Heymsfield (2005), Production of ice in tropospheric clouds: A review, *Bull. Am. Meteorol. Soc.*, *86*(6), 795–807, doi:10.1175/BAMS-86-6-795.

Carvalho, A., C. Pio, and C. Santos (2003), Water-soluble hydroxylated organic compounds in German and Finnish aerosols, *Atmos. Environ.*, *37*, 1775–1783, doi:10.1016/S1352-2310(03)00066-9.

Chernoff, D. I., and A. K. Bertram (2010), Effects of sulfate coatings on the ice nucleation properties of a biological ice nucleus and several types of minerals, *J. Geophys. Res.*, *115*, D20205, doi:10.1029/2010JD014254.

Claeys, M., et al. (2010), Polar organic marker compounds in atmospheric aerosols during the LBA-SMOCC 2002 biomass burning experiment in Rondônia, Brazil: Sources and source processes, time series, diel variations and size distributions, *Atmos. Chem. Phys.*, *10*, 9319–9331, doi:10.5194/acp-10-9319-2010.

Cozic, J., S. Mertes, B. Verheggen, D. J. Cziczo, S. J. Gallavardin, S. Walter, U. Baltensperger, and E. Weingartner (2008), Black carbon enrichment in atmospheric ice particle residuals observed in lower tropospheric mixed phase clouds, *J. Geophys. Res.*, *113*, D15209, doi:10.1029/2007JD009266.

Crawford, I., et al. (2011), Studies of propane flame soot acting as heterogeneous ice nuclei in conjunction with single particle soot photometer measurements, *Atmos. Chem. Phys. Discuss.*, *11*, 11,007–11,038, doi:10.5194/acpd-11-11007-2011.

Cruz, C. N., and S. N. Pandis (1997), A study of the ability of pure secondary organic aerosol to act as cloud condensation nuclei, *Atmos. Environ.*, *31*(15), 2205–2214, doi:10.1016/S1352-2310(97)00054-X.

Cziczo, D. J., P. J. DeMott, S. D. Brooks, A. J. Prenni, D. S. Thomson, D. Baumgardner, J. C. Wilson, S. M. Kreidenweis, and D. M. Murphy (2004), Observations of organic species and atmospheric ice formation, *Geophys. Res. Lett.*, *31*, L12116, doi:10.1029/2004GL019822.

DeMott, P. J. (1990), An exploratory study of ice nucleation by soot aerosols, *J. Appl. Meteorol.*, *29*, 1072–1079, doi:10.1175/1520-0450(1990)029<1072:AESOIN>2.0.CO;2.

DeMott, P. J., Y. Chen, S. M. Kreidenweis, D. C. Rogers, and D. E. Sherman (1999), Ice formation by black carbon particles, *Geophys. Res. Lett.*, *26*(16), 2429–2432, doi:10.1029/1999GL900580.

DeMott, P. J., D. J. Cziczo, A. J. Prenni, D. M. Murphy, S. M. Kreidenweis, D. S. Thomson, R. Borys, and D. C. Rogers (2003), Measurements of the concentration and composition of nuclei for cirrus formation, *Proc. Natl. Acad. Sci. U. S. A.*, *100*(25), 14,655–14,660, doi:10.1073/pnas.2532677100.

Diehl, K., and S. K. Mitra (1998), A laboratory study of the effects of a kerosene-burner exhaust on ice nucleation and the evaporation rate of ice crystals, *Atmos. Environ.*, *32*(18), 3145–3151, doi:10.1016/S1352-2310(97)00467-6.

Dymarska, M., B. J. Murray, L. Sun, M. L. Eastwood, D. A. Knopf, and A. K. Bertram (2006), Deposition ice nucleation on soot at temperatures relevant for the lower troposphere, *J. Geophys. Res.*, *111*, D04204, doi:10.1029/2005JD006627.

Eastwood, M. L., S. Cremel, C. Gehrke, E. Girard, and A. K. Bertram (2008), Ice nucleation on mineral dust particles: Onset conditions, nucleation rates and contact angles, *J. Geophys. Res.*, *113*, D22203, doi:10.1029/2008JD010639.

Ebert, M., A. Worringen, N. Benker, S. Mertes, E. Weingartner, and S. Weinbruch (2010), Chemical composition and mixing-state of ice residuals sampled within mixed phase clouds, *Atmos. Chem. Phys. Discuss.*, *10*, 23,865–23,894, doi:10.5194/acpd-10-23865-2010.

Fletcher, N. H. (1958), Size effect in heterogeneous nucleation, *J. Chem. Phys.*, *29*(3), 572–576, doi:10.1063/1.1744540.

Forster, P., et al. (2007), Changes in atmospheric constituents and in radiative forcing, in *Climate Change 2007: The Physical Science Basis. Contribution of Working Group I to the Fourth Assessment Report of the Intergovernmental Panel on Climate Change*, edited by S. Solomon et al., Cambridge Univ Press, Cambridge, U. K.

Gorbunov, B., A. Baklanov, N. Kakutkina, H. L. Windsor, and R. Toumi (2001), Ice nucleation on soot particles, *J. Aerosol Sci.*, *32*, 199–215, doi:10.1016/S0021-8502(00)00077-X.

Hearn, J. D., and G. D. Smith (2005), Measuring rates of reaction in supercooled organic particles with implications for atmospheric aerosol, *Phys. Chem. Chem. Phys.*, *7*, 2549–2551, doi:10.1039/b506424d.

Hings, S. S., W. C. Wrobel, E. S. Cross, D. R. Worsnop, P. Davidovits, and T. B. Onasch (2008), CCN activation experiments with adipic acid: Effect of particle phase and adipic acid coatings on soluble and insoluble particles, *Atmos. Chem. Phys.*, *8*, 3735–3748, doi:10.5194/acp-8-3735-2008.

Hsieh, L. Y., S.-C. Kuo, C.-L. Chen, and Y. I. Tsai (2007), Origin of low-molecular-weight dicarboxylic acids and their concentration and size distribution variation in suburban aerosol, *Atmos. Environ.*, *41*(31), 6648–6661, doi:10.1016/j.atmosenv.2007.04.014.

Kanji, Z. A., and J. P. D. Abbatt (2006), Laboratory studies of ice formation via deposition mode nucleation onto mineral dust and n-hexane soot samples, *J. Geophys. Res.*, *111*, D16204, doi:10.1029/2005JD006766.

Kärcher, B. (1996), The initial composition of jet condensation trails, *J. Atmos. Sci.*, *53*(21), 3066–3083, doi:10.1175/1520-0469(1996)053<3066:TICOJC>2.0.CO;2.

Kärcher, B., and U. Lohmann (2003), A parameterization of cirrus cloud formation: Heterogeneous freezing, *J. Geophys. Res.*, *108*(D14), 4402, doi:10.1029/2002JD003220.

Kärcher, B., O. Möhler, P. J. DeMott, S. Pechtl, and F. Yu (2007), Insights into the role of soot aerosols in cirrus cloud formation, *Atmos. Chem. Phys.*, *7*, 4203–4227, doi:10.5194/acp-7-4203-2007.

Kawamura, K., R. Seméré, Y. Imai, Y. Fujii, and M. Hayashi (1996), Water-soluble dicarboxylic acids and related compounds in Antarctic aerosols, *J. Geophys. Res.*, *101*(D13), 18,721–18,728, doi:10.1029/96JD01541.

Khalizov, A. F., R. Zhang, D. Zhang, H. Xue, J. Pagels, and P. H. McMurry (2009), Formation of highly hygroscopic soot aerosols upon internal mixing with sulfuric acid vapor, *J. Geophys. Res.*, *114*, D05208, doi:10.1029/2008JD010595.

Koehler, K. A., P. J. DeMott, S. M. Kreidenweis, O. B. Popovicheva, M. D. Petters, C. M. Carrico, E. D. Kireeva, T. D. Khokhlova, and N. K. Shonija (2009), Cloud condensation nuclei and ice nucleation activity of hydrophobic and hydrophilic soot particles, *Phys. Chem. Chem. Phys.*, *11*, 7906–7920, doi:10.1039/b905334b.

Koop, T., B. Luo, A. Tsias, and T. Peter (2000), Water activity as the determinant for homogeneous ice nucleation in aqueous solutions, *Nature*, *406*, 611–614, doi:10.1038/35020537.

Lance, S., J. Medina, J. N. Smith, and A. Nenes (2006), Mapping the operation of the DMT continuous flow CCN counter, *Aerosol Sci. Technol.*, *40*, 242–254, doi:10.1080/02786820500543290.

Lohmann, U. (2002), A glaciation indirect aerosol effect caused by soot aerosols, *Geophys. Res. Lett.*, *29*(4), 1052, doi:10.1029/2001GL014357.

Lohmann, U., and K. Diehl (2006), Sensitivity studies of the importance of dust ice nuclei for the indirect aerosol effect on stratiform mixed-phase clouds, *J. Atmos. Sci.*, *63*, 968–982, doi:10.1175/JAS3662.1.

Maria, S. F., L. M. Russell, M. K. Gilles, and S. C. B. Myneni (2004), Organic aerosol growth mechanisms and their climate-forcing implications, *Science*, *306*, 1921–1924, doi:10.1126/science.1103491.

Meyers, M. P., P. J. DeMott, and W. R. Cotton (1992), New primary ice-nucleation parameterizations in an explicit cloud model, *J. Appl. Meteorol.*, *31*, 708–721, doi:10.1175/1520-0450(1992)031<0708:NPINPI>2.0.CO;2.

Möhler, O., et al. (2005a), Effect of sulfuric acid coating on heterogeneous ice nucleation by soot aerosol particles, *J. Geophys. Res.*, *110*, D11210, doi:10.1029/2004JD005169.

Möhler, O., C. Linke, H. Saathoff, M. Schnaiter, R. Wagner, A. Mangold, M. Krämer, and U. Schurath (2005b), Ice nucleation on flame soot aerosol of different organic carbon content, *Meteorol. Z.*, *14*(4), 477–484, doi:10.1127/0941-2948/2005/0055.

Murphy, D. M., D. J. Cziczo, K. D. Froyd, P. K. Hudson, B. M. Matthew, A. M. Middlebrook, R. E. Peltier, A. Sullivan, D. S. Thomson, and R. J. Weber (2006), Single-particle mass spectrometry of tropospheric aerosol particles, *J. Geophys. Res.*, *111*, D23S32, doi:10.1029/2006JD007340.

Murray, B. J. (2008), Inhibition of ice crystallisation in highly viscous aqueous organic acid droplets, *Atmos. Chem. Phys.*, *8*, 5423–5433, doi:10.5194/acp-8-5423-2008.

Murray, B. J., et al. (2010), Heterogeneous nucleation of ice particles on glassy aerosols under cirrus conditions, *Nat. Geosci.*, *3*, 233–237, doi:10.1038/ngeo817.

Petters, M. D., et al. (2009), Ice nuclei emissions from biomass burning, *J. Geophys. Res.*, *114*, D07209, doi:10.1029/2008JD011532.

Phillips, V. T. J., P. J. DeMott, and C. Andronache (2008), An empirical parameterization of heterogeneous ice nucleation for multiple chemical species of aerosol, *J. Atmos. Sci.*, *65*, 2757–2783, doi:10.1175/2007JAS2546.1.

Popovicheva, O., N. M. Persiantseva, N. K. Shonija, P. DeMott, K. Koehler, M. Petters, S. Kreidenweis, V. Tishkova, B. Demirdjian, and J. Suzanne (2008), Water interaction with hydrophobic and hydrophilic soot particles, *Phys. Chem. Chem. Phys.*, *10*, 2332–2344, doi:10.1039/b718944n.

Popovicheva, O. B., E. D. Kireeva, N. K. Shonija, and T. D. Khokhlova (2009), Water interaction with laboratory-simulated fossil fuel combustion particles, *J. Phys. Chem. A*, *113*, 10,503–10,511, doi:10.1021/jp905522s.

Popovicheva, O. B., N. M. Persiantseva, E. D. Kireeva, T. D. Khokhlova, and N. K. Shonija (2011), Quantification of the hygroscopic effect of soot aging in the atmosphere: Laboratory simulations, *J. Phys. Chem. A*, *115*, 298–306, doi:10.1021/jp109238x.

Pruppacher, H. R., and J. D. Klett (1997), *Microphysics of Clouds and Precipitation*, 2nd ed., 954 pp., Kluwer Acad., Dordrecht, Netherlands.

Richardson, M. S., et al. (2007), Measurements of heterogeneous ice nuclei in the western United States in springtime and their relation to aerosol characteristics, *J. Geophys. Res.*, *112*, D02209, doi:10.1029/2006JD007500.

Riemer, N., H. Vogel, and B. Vogel (2004), Soot aging time scales in polluted regions during day and night, *Atmos. Chem. Phys.*, *4*, 1885–1893, doi:10.5194/acp-4-1885-2004.

Rissman, T. A., V. Varutbangkul, J. D. Surratt, D. O. Topping, G. McFiggans, R. C. Flagan, and J. H. Seinfeld (2007), Cloud condensation nucleus (CCN) behavior of organic aerosol particles generated by atomization of water and methanol solutions, *Atmos. Chem. Phys.*, *7*, 2949–2971, doi:10.5194/acp-7-2949-2007.

Roberts, G. C., and A. Nenes (2005), A continuous-flow streamwise thermal-gradient CCN chamber for atmospheric measurements, *Aerosol Sci. Technol.*, *39*, 206–221, doi:10.1080/027868290913988.

Roberts, P., and J. Hallett (1968), A laboratory study of the ice nucleating properties of some mineral particulates, *Q. J. R. Meteorol. Soc.*, *94*(399), 25–34, doi:10.1002/qj.49709439904.

Salam, A., U. Lohmann, and G. Lesins (2007), Ice nucleation of ammonia gas exposed montmorillonite mineral dust particles, *Atmos. Chem. Phys.*, *7*, 3923–3931, doi:10.5194/acp-7-3923-2007.

Saxena, P., and L. M. Hildemann (1996), Water-soluble organics in atmospheric particles: A critical review of the literature and application of thermodynamics to identify candidate compounds, *Atmos. Chem. Phys.*, *24*(1), 57–109, doi:10.1007/BF00053823.

Seinfeld, J. H., and S. N. Pandis (2006), *Atmospheric Chemistry and Physics: From Air Pollution to Climate Change*, 2nd ed., John Wiley, Hoboken, N. J.

Sempére, R., and K. Kawamura (1994), Comparative distributions of dicarboxylic acids and related polar compounds in snow, rain and aerosols from urban atmosphere, *Atmos. Environ.*, *28*(3), 449–459, doi:10.1016/1352-2310(94)90123-6.

Shilling, J. E., T. J. Fortin, and M. A. Tolbert (2006), Depositional ice nucleation on crystalline organic and inorganic solids, *J. Geophys. Res.*, *111*, D12204, doi:10.1029/2005JD006664.

Slowik, J. G., E. S. Cross, J.-H. Han, J. Kolucki, P. Davidovits, L. R. Williams, T. B. Onasch, J. T. Jayne, C. E. Kolb, and D. R. Worsnop (2007), Measurements of morphology changes of fractal soot particles using coating and denuding experiments: Implications for optical absorption and atmospheric lifetime, *Aerosol Sci. Technol.*, *41*(8), 734–750, doi:10.1080/02786820701432632.

Stetzer, O., B. Baschek, F. Lüönd, and U. Lohmann (2008), The Zurich Ice Nucleation Chamber (ZINC)—A new instrument to investigate atmospheric ice formation, *Aerosol Sci. Technol.*, *42*(1), 64–74, doi:10.1080/02786820701787944.

Weingartner, E., H. Burtscher, and U. Baltensperger (1997), Hygroscopic properties of carbon and diesel soot particles, *Atmos. Environ.*, *31*(15), 2311–2327, doi:10.1016/S1352-2310(97)00023-X.

Welti, A., F. Lüönd, O. Stetzer, and U. Lohmann (2009), Influence of particle size on the ice nucleating ability of mineral dusts, *Atmos. Chem. Phys.*, *9*, 6705–6715, doi:10.5194/acp-9-6705-2009.

Zelenyuk, A., and D. Imre (2005), Single particle laser ablation time-of-flight mass spectrometer: An introduction to SPLAT, *Aerosol Sci. Technol.*, *39*(6), 554–568, doi:10.1080/027868291009242.

Zelenyuk, A., and D. Imre (2009), Beyond single particle mass spectrometry: Multidimensional characterisation of individual aerosol particles, *Int. Rev. Phys. Chem.*, *28*(2), 309–358, doi:10.1080/01442350903037458.

Zhang, R., A. F. Khalizov, J. Pagels, D. Zhang, H. Xue, and P. H. McMurry (2008), Variability in morphology, hygroscopicity, and optical properties of soot aerosols during atmospheric processing, *Proc. Natl. Acad. Sci. U. S. A.*, *105*(30), 10,291–10,296, doi:10.1073/pnas.0804860105.

Zobrist, B., C. Marcolli, D. A. Pedernera, and T. Koop (2008), Do atmospheric aerosols form glasses?, *Atmos. Chem. Phys.*, *8*, 5221–5244, doi:10.5194/acp-8-5221-2008.

J. Beránek, G. Kulkarni, and A. Zelenyuk, Pacific Northwest National Laboratory, Richland, WA 99352, USA.

D. J. Cziczo, Department of Earth, Atmospheric, and Planetary Sciences, Massachusetts Institute of Technology, Cambridge, MA 02139, USA. (djcziczo@mit.edu)

B. Friedman and J. A. Thornton, Department of Atmospheric Sciences, University of Washington, Seattle, WA 98195, USA.